Liquid Crystals

Publication details, including instructions for authors and subscription information:
http://www.informaworld.com/smpp/title~content=t713926090

Synthesis and characterisation of unsymmetrical six-aromatic ring containing bent-shaped compounds

K. C. Majumdar[a]; P. K. Shyam[a]; S. Chakravorty[a]
[a] Department of Chemistry, University of Kalyani, Kalyani, India

To cite this Article Majumdar, K. C. , Shyam, P. K. and Chakravorty, S.(2010) 'Synthesis and characterisation of unsymmetrical six-aromatic ring containing bent-shaped compounds', Liquid Crystals, 37: 10, 1237 — 1243

To link to this Article: DOI: 10.1080/02678292.2010.495793

URL: http://dx.doi.org/10.1080/02678292.2010.495793

Liquid Crystals,
Vol. 37, No. 10, October 2010, 1237–1243

Synthesis and characterisation of unsymmetrical six-aromatic ring containing bent-shaped compounds

K.C. Majumdar*, P.K. Shyam and S. Chakravorty

Department of Chemistry, University of Kalyani, Kalyani, India

(*Received 1 January 2010; final version received 20 May 2010*)

A new series of achiral unsymmetrical six-aromatic ring banana-shaped compounds has been synthesised and characterised by polarising optical microscopy, differential scanning calorimetry and X-ray diffraction. The lower homologue (C_6) exhibits an intercalated B6 phase. The middle homologues (C_{10}, C_{12}) form only a B1 phase while higher homologues (C_{14}, C_{16}, C_{18}) exhibit a B2 mesophase.

Keywords: unsymmetrical bent-shaped mesogen; Schiff's base; B2 phase; B1 phase; B6 phase

1. Introduction

Liquid crystals are partially ordered, anisotropic fluids, thermodynamically located between the solid state and isotropic liquid. Liquid crystalline phases represent intriguing states of soft matter, combining order and mobility on a molecular level [1]. These unique phases create fascinating systems which respond to external stimuli by finding a new configuration [2, 3]. Thus, liquid crystalline materials have had a major impact on the recent development of mobile information technologies, with numerous applications in optoelectric devices.

The vast majority of liquid crystalline compounds are either rod-like or disc-like in shape. They generally exhibit a lamellar and/or columnar mesophase. Since the discovery of the unique feature of achiral bent-core molecules of the formation of a polar order mesophase [4–7], extensive investigations have been made to synthesise this type of material. Mesogens built of bent-shaped molecules represent a distinct class of thermotropic liquid crystals, as they can form a new type of mesophase with no analogues among classical calamatic phases [8, 9]. Most of the phases formed by banana-mesogens have an antiferroelectric interlayer structure [10, 11]. Only in special cases when the bent-shaped molecules contain chiral centres in the terminal chains or different terminal chains in each banana branch is the ferroelectric ground state obtained [12, 13].

The bent-shaped molecules generally exhibit Bn phases. An antiferroelectric fluid smectic phase is referred to as B2 phase. The B5 smectic phase possesses an additional short-range order within the layers [14]. In intercalated smectic phase labelled B6, the layer spacing is less than half the length of the molecules. On the other hand, monolayer smectic phases are referred to as B1 in the case of bent-shaped molecules [15].

Most of the bent-shaped molecules so far synthesised are symmetrical in nature, though limited numbers of examples of unsymmetrical bent-core molecules are reported in the literature [16, 17]. Symmetrical bent-core molecules comprising an angular central core substituted with two identical linear rod-like mesogenic segments generally exhibit higher transition temperatures than unsymmetrical bent-core molecules [16, 17]. To reduce the transition temperatures and to perhaps bridge the gap between bent-core and rod-like liquid crystals, non-symmetrical bent-core molecules have been designed and synthesised [18]. In these molecules, either the two halves of the molecule or the linking functional groups attached to one angular central core are different.

In continuation of our efforts to synthesise bent-shaped materials [19–21] and to realise their structure–property relationship, we have undertaken a study to synthesise a series of unsymmetrical bent-shaped materials having six aromatic rings.

2. Experimental methods

All the chemicals were procured from either Sigma Aldrich Chemicals Pvt. Ltd or Spectrochem, India. Silica gel (60–120 mesh) was used for chromatographic separation. Silica gel G (E-Merck, India) was used for TLC. Petroleum ether refers to the fraction boiling between 60°C and 80°C. IR spectra were recorded on a Perkin-Elmer L 120-000A spectrometer ($\nu_{\max}$ in cm^{-1}) on KBr discs. ^{1}H NMR (300 MHz, 400 MHz) spectra were recorded on Bruker DPX-300 and Bruker DPX-400 spectrometers in $CDCl_3$ (chemical shift in δ) with TMS as internal standard. Chemical analysis was performed on a 2400 series II CHN analyser (Perkin Elmer). The liquid crystalline properties

---

*Corresponding author. Email: kcm_ku@yahoo.co.in

ISSN 0267-8292 print/ISSN 1366-5855 online

DOI: 10.1080/02678292.2010.495793
http://www.informaworld.com

were established by thermal microscopy (Nikon polarising microscope LV100POL attached with Instec hot and cold stage HCS302, with STC200 temperature controller configured for HCS302) and the phase transitions were confirmed by differential scanning calorimetry (Perkin-Elmer Diamond DSC system).

*2.1 General procedure for the preparation of 4-[(3-aminophenoxy)carbonyl]phenyl 4-(*n*-alkyloxy) benzoate, 5a-f*

These were prepared according to a published procedure [18].

2.2 General procedure for the formation of aldehydes, 6a–f

A mixture of 4-(4-(hexadecyloxy)benzoyloxy)benzoic acid **3b** (500 mg, 0.99 mmol) and $SOCl_2$ was stirred at 100°C for 3 h. After evaporation of the solvent, the residue was dissolved in CH_2Cl_2 (20 mL). A solution of 4-hydroxybenzaldehyde (121 mg, 0.99 mmol) in CH_2Cl_2 (20 mL) and tetrabutyl ammonium hydrogen sulphate (catalytic amount) was added to the stirred solution of the acid chloride. To this reaction mixture an aqueous solution of K_2CO_3 (274 mg, 1.98 mmol) was slowly added. After stirring for 4 h at room temperature, the solution was washed with 5% HCl (2 × 20 ml) and then with 5% aqueous NaOH (2 × 20 ml). The organic layer was dried (Na_2SO_4) and the solvent was evaporated under reduced pressure. The residue was purified by column chromatography over silica gel using petroleum ether–ethyl acetate (9:1) as an eluent to give aldehyde **6b**. The aldehydes **6a** and **6c–f** were prepared accordingly.

2.2.1 Compound 6a

Yield: 80%; white solid; IR (KBr, cm^{-1}): ν_{max}: 2914, 1741, 1702, 1601 cm^{-1}; ^1H NMR ($CDCl_3$, 400 MHz): $\delta_H = 10.04$ (s, 1H), 8.26 (m, 2H), 8.13 (m, 2H), 7.98 (m, 2H), 7.39 (m, 4H), 6.97 (m, 2H), 4.03 (t, 2H, $J = 6.8$ Hz), 1.82 (q, 2H, $J = 6.8$ Hz), 0.87–1.57 (m, 33H).

2.2.2 Compound 6b

Yield: 81%; white solid; IR (KBr, cm^{-1}): ν_{max}: 2916, 1743, 1703, 1604 cm^{-1}; ^1H NMR ($CDCl_3$, 400 MHz): $\delta_H = 10.03$ (s, 1H), 8.27 (m, 2H), 8.14 (m, 2H), 7.98 (m, 2H), 7.38(m, 4H), 6.98 (m, 2H), 4.04 (t, 2H, $J = 6.4$ Hz), 1.81 (q, 2H, $J = 7.2$ Hz), 0.86–1.58 (m, 29H).

2.2.3 Compound 6c

Yield: 83%; white solid; IR (KBr, cm^{-1}): ν_{max}: 2917, 1735, 1702, 1603; ^1H NMR ($CDCl_3$, 400 MHz): $\delta_H =$ 10.03 (s, 1H), 8.27 (m, 2H), 8.13 (m, 2H), 7.97 (m, 2H), 7.37 (m, 4H), 6.97 (m, 2H), 4.04 (t, 2H, $J = 6.4$ Hz), 1.79 (q, 2H, $J = 6.8$ Hz), 0.86–1.58 (m, 25H).

2.2.4 Compound 6d

Yield: 87%; white solid; IR (KBr, cm^{-1}): ν_{max}: 2918, 1733, 1699, 1603 cm^{-1}; ^1H NMR ($CDCl_3$, 400 MHz): $\delta_H = 10.04$ (s, 1H), 8.26 (m, 2H), 8.14 (m, 2H), 7.97 (m, 2H), 7.38 (m, 4H), 6.98 (m, 2H), 4.04 (t, 2H, $J = 6.8$ Hz), 1.86 (q, 2H, $J = 6.8$ Hz), 0.87–1.57 (m, 21H).

2.2.5 Compound 6e

Yield: 85%; white solid; IR (KBr, cm^{-1}): ν_{max}: 2917, 1741, 1705, 1605 cm^{-1}; ^1H NMR ($CDCl_3$, 400 MHz): $\delta_H = 9.96$ (s, 1H), 8.19 (m, 2H), 8.06 (m, 2H), 7.90 (m, 2H), 7.30 (m, 4H), 6.90 (m, 2H), 3.97 (t, 2H, $J = 6.4$ Hz), 1.72 (q, 2H, $J = 6.4$ Hz), 0.80–1.56 (m, 17H).

2.2.6 Compound 6f

Yield: 90%; white solid; IR (KBr, cm^{-1}): ν_{max}: 2920, 1734, 1703, 1605 cm^{-1}; ^1H NMR ($CDCl_3$, 400 MHz): $\delta_H = 10.03$ (s, 1H), 8.27 (d, 2H, $J = 8.8$ Hz), 8.14 (d, 2H, $J = 8.4$ Hz), 7.97 (d, 2H, $J = 8.8$ Hz), 7.41 (d, 2H, $J = 8.4$ Hz), 7.38 (d, 2H, $J = 8.4$ Hz), 6.98 (d, 2H, $J = 8.8$ Hz), 4.04 (t, 2H, $J = 6.4$ Hz), 1.81 (q, 2H, $J = 6.8$ Hz), 0.90–1.57 (m, 9H).

2.3 General procedure for the Schiff's base formation, 7a–f

A mixture of 4-[(3-aminophenoxy)carbonyl]phenyl 4-(*n*-octadecyloxy)benzoate **5a** (0.1 g, 0.17 mmol) and 4-(4-formylbenzoyloxy)phenyl 4-(*n*-octadecyloxy)benzoate **6a** (0.1 g, 0.17 mmol) was refluxed in absolute ethanol (10 mL) in the presence of a catalytic amount of glacial acetic acid for 12 h. The Schiff's base **7a** was precipitated out from the reaction mixture. The solid material was collected, washed repeatedly with hot ethanol and dried in vacuum. The other derivatives **7b–f** were prepared similarly.

2.3.1 Compound 7a

Yield: 90%; white solid; IR (KBr): $\upsilon = 2918$, 2849, 1730,1634, 1604 cm^{-1}; ^1H NMR ($CDCl_3$, 400 MHz): $\delta_H = 8.51$ (s, 1H), 8.28 (dd, 4H, $J = 1.2$ Hz, 8.4 Hz), 8.14 (d, 4H, $J = 9.2$ Hz), 7.99 (d, 2H, $J = 8.4$ Hz,), 7.35–7.46 (m, 7H), 7.11–7.16 (m, 3H), 6.98 (d, 4H, $J =$ 8.8 Hz), 4.04 (t, 4H, J =6.4 Hz), 1.81 (q, 4H, J = 7.6 Hz), 0.82–1.50 (m, 66H), ppm. Analysis (%) calculated for $C_{77}H_{99}NO_{10}$: C = 77.16, H = 8.33, N = 1.17; found: C = 77.40, H = 8.54, N = 1.25.

2.3.2 *Compound 7b*

Yield: 95%; white solid; IR (KBr): υ = 2920, 2851, 1730, 1630, 1603 cm^{-1}; ^{1}H NMR (CDCl$_3$, 400 MHz): δ_H = 8.51 (s, 1H), 8.28 (d, 4H, J = 8.8Hz), 8.14 (d, 4H, J = 8.8 Hz), 7.99 (d, 2H, J = 8.4 Hz), 7.44 (t, 1H, J = 8.4 Hz), 7.35–7.39 (m, 6H), 7.11–7.16 (m, 3H), 6.98 (d, 4H, J = 8.8 Hz), 4.03 (t, 4H, J =6.8Hz), 1.79 (q, 4H, J = 6.8 Hz), 0.86-–1.50 (m, 58H) ppm; ^{13}C NMR (100 MHz): 164.4, 164.3, 164.1, 163.8, 159.9, 155.6, 155.4, 153.4, 153.2, 151.5, 133.8, 132.4, 131.9, 131.8, 130.2, 129.9, 126.8, 126.5, 122.3, 122.2, 122.1, 120.9, 119.1, 118.9, 114.4, 114.2, 68.4, 31.9, 29.8, 29.7, 29.6, 29.5, 29.4, 29.1, 26.0, 22.7, 14.1 ppm. Analysis (%) calculated for $C_{73}H_{91}NO_{10}$: C = 76.74, H = 8.03, N = 1.23; found: C = 76.99, H = 8.24, N = 1.30.

2.3.3 *Compound 7c*

Yield: 96%; white solid; IR (KBr): υ = 2919, 2850, 1732, 1634, 1605 cm^{-1}; ^{1}H NMR (CDCl$_3$, 400 MHz): δ_H = 8.51 (s, 1H), 8.28 (dd, 4H, J = 1.2 Hz, 8.8 Hz), 8.14 (d, 4H, J = 8.8 Hz), 7.99 (d, 2H, J = 8.8 Hz,), 7.44 (t, 1H, J = 8.4 Hz), 7.35-7.40 (m, 6H), 7.11-7.16 (m, 3H), 6.98 (d, 4H, J = 8.4 Hz), 4.04 (t, 4H, J =6.4 Hz), 1.79 (q, 4H, J = 6.4 Hz), 0.86-1.51 (m, 50H) ppm. Analysis (%) calculated for $C_{69}H_{83}NO_{10}$: C = 76.28, H = 7.70, N = 1.29; found: C = 76.40, H = 7.96, N = 1.25.

2.3.4 *Compound 7d*

Yield: 95%; white solid; IR (KBr): υ = 2919, 2853, 1738, 1730, 1629, 1605 cm^{-1}; ^{1}H NMR (CDCl$_3$, 300 MHz): δ_H = 8.51 (s, 1H), 8.28 (d, 4H, J = 8.4Hz), 8.14 (d, 4H, J = 8.7 Hz), 7.98 (d, 2H, J = 8.1 Hz), 7.43 (t, 1H, J= 8.1 Hz), 7.37–7.39 (m, 6H), 7.11–7.17 (m, 3H), 6.97 (d, 4H, J = 8.4 Hz), 4.03 (t, 4H, J =6.3 Hz), 1.80 (q, 4H, J = 6.6 Hz), 0.86–1.85 (m, 42H); ^{13}C NMR (100 MHz): 164.4, 164.3, 164.1, 163.8, 159.9, 155.4, 151.5, 133.7, 132.4, 131.9, 131.8, 131.3, 130.2, 129.9, 126.6, 122.3, 122.6, 122.3, 122.2, 122.1, 120.9, 118.9, 114.4, 114.2, 68.4, 31.9, 29.7, 29.6, 29.4, 29.1, 26.0, 22.7, 14.1 ppm. Analysis (%) calculated for $C_{65}H_{75}NO_{10}$: C = 75.77, H = 7.34, N = 1.36; found: C = 75.94, H = 7.55, N = 1.45.

2.3.5 *Compound 7e*

Yield: 96%; white solid; IR (KBr): υ = 2922, 2852, 1735, 1627, 1605 cm^{-1}; ^{1}H NMR (CDCl$_3$, 400 MHz): δ_H = 8.51 (s, 1H), 8.28 (d, 4H, J = 8.4 Hz), 8.14 (d, 4H, J = 8.4 Hz), 7.99 (d, 2H, J = 8.4 Hz,), 7.44 (t, 1H, J = 8.0 Hz), 7.35–7.39 (m, 6H), 7.11–7.16 (m, 3H), 6.98 (d, 4H, J = 8.8 Hz), 4.04 (t, 4H, J =6.8 Hz), 1.79 (q, 4H, J = 6.4 Hz), 0.88–1.49 (m, 34H) ppm. Analysis (%) calculated $C_{61}H_{67}NO_{10}$: C = 75.21, H = 6.93, N = 1.44; found: C = 75.40, H = 7.14, N = 1.43.

2.3.6 *Compound 7f*

Yield: 98%; white solid; IR (KBr): υ = 2951, 1732, 1629, 1605 cm^{-1}; ^{1}H NMR (CDCl$_3$, 400 MHz): δ_H = 8.51 (s, 1H), 8.28 (d, 4H, J = 8.4 Hz), 8.14 (d, 4H, J = 8.7 Hz), 7.98 (d, 2H, J = 8.7 Hz,), 7.43 (t, 1H, J = 8.4 Hz), 7.35-7.39 (m, 6H), 7.11-7.17 (m, 3H), 6.97 (d, 4H, J = 8.7 Hz), 4.03 (t, 4H, J =6.3 Hz), 1.78 (q, 4H, J = 6.6 Hz), 0.92–1.52 (m, 18H) ppm. Analysis (%) calculated for $C_{53}H_{51}NO_{10}$: C = 73.85, H = 5.96, N = 1.62; found: C = 74.10, H = 6.04, N = 1.71.

3. Results and discussion

The aforesaid series of unsymmetrical banana-shaped materials **7a–f** were prepared by the acid catalysed condensation of the key intermediate namely 4-(4-formylbenzoyloxy)phenyl 4-(alkyloxy)benzoates with amines **5** in ethanol as depicted in Scheme 1. The intermediate **6** was obtained by esterification of **3** with 4-hydroxybenzaldehyde. Amines **5** were prepared in five steps starting from 4-(*n*-alkyloxy) benzoic acid **1**. The phase transition temperatures and the corresponding enthalpy changes of all the compounds obtained from differential scanning calorimetry (DSC) are summarised in Table 1.

Only one mesophase was observed for each compound in the series; either monotropic or enantiotropic phase behaviour was observed. The mesomorphic behaviour is significantly influenced by the terminal alkoxy flexible chain. All the compounds bearing the longest chain length (C_{14}, C_{16}, C_{18}) show the B2 phase. Middle members of the homologous series (compounds C_{12}, C_{10}) show a B1 phase (C_{12} is enantiotropic while C_{10} is monotropic in nature), while the lowest members of the series (C_6) show a B6 phase [22].

The DSC scan of compounds **7a–c** exhibited some solid–solid phase transitions in addition to crystal–liquid crystalline phase transitions and liquid crystalline phase–isotropic phase transitions. These types of transitions were observed only in the DSC scan of compounds **7a–c** in the heating cycles. When sandwiched between two glass plates, compound **7b** displays a stripe-like texture appearing from the isotropic melt, which on further cooling grows slowly and fills up the whole field of view with circular domains (Figure 1). This is a typical texture of a B2 phase [23]. All the other higher homologues (C_{14}, C_{18}) exhibit a similar type of texture.

The B1 phase exhibits both mosaic-like textures and dendritic nuclei textures as it grows from the isotropic melt. As the temperature is lowered, the

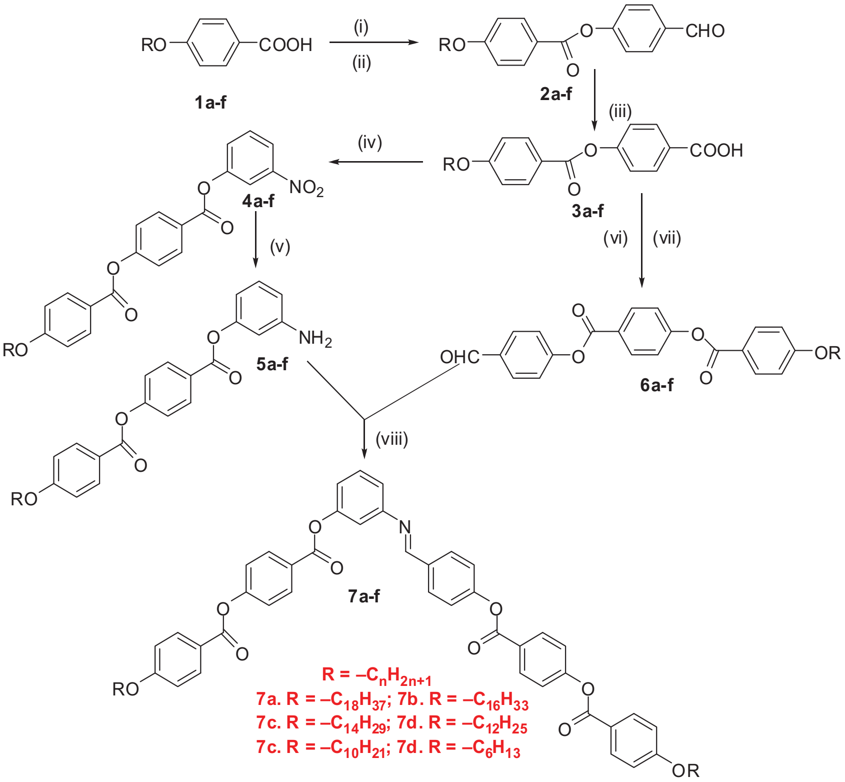

Scheme 1. Reagents and conditions: (i) $SOCl_2$ reflux, 4 hrs (ii) *p*-hydroxy benzaldehyde, CH_2Cl_2, DMAP, NEt_3, rt, 4 hr (iii) CrO_3, $H_2SO_4/H_2O(1{:}3)$ (iv) *m*-nitrophenol, CH_2Cl_2, DCC, DMAP (v) H_2, Pd-C, ethyl acetate (vi) $SOCl_2$ reflux, 2 hrs (vii) *p*-hydroxy benzaldehyde, DCM, aq K_2CO_3, Bu_4NHSO_4, 4 h (vii) anhydrous alcohol, AcOH (Cat), reflux, 12 h.

dendritic nucleus rapidly coalesces into a mosaic-like structure with some spherulitic domains. The typical mosaic-like textures [18] of the B1 phase of compound **7d** at 129°C is presented in Figure 2. Similar textural features of the B1 phase were observed with compound **7e**. The transition enthalpies of the B1 isotropic transition are in the range 18.8–19.0 kJ mol^{-1}.

The lower homologue (C_6) of the series (**7f**) exhibits the fan-like textures of a SmA phase but without any homeotropic tendency. If it was a SmA phase, then it must have exhibited homeotropic behaviour when it was placed between two glass plates and was observed perpendicularly. Therefore this may be the typical characteristic textures of the B6 phase [22]. The fan-like texture of compound **7f** at 160°C is presented in Figure 3.

The X-ray diffraction diagram (Figure 4) of compound **7b** [23] shows three sharp lamellar reflection peaks in the small angle region with a 2θ value of 2.08 (d_1 = 42.43 Å), 4.02 (d_2 = 21.96 Å) and 5.98 (d_3 =14.77 Å), respectively, and a broad diffuse peak in the wide angle region centred at d-spacing of 4.58 Å due to the liquid-like co-relation of the molecules. The molecular length (L = 65.86 Å) was calculated by molecular modelling (by DFT = B3LYP calculation using 6–31G basis set), assuming the molecules have a fully stretched conformation. The first order reflection is found to be at d = 42.43 Å, which is sufficiently smaller than the molecular length L and hence the molecules are assumed to be tilted within the layers. From X-ray diffraction, molecular modelling and textural observation, the mesophase of **7b** is characterised as B2.

The X-ray diffraction diagram (Figure 5) of the mesophase of compound **7d** at 140°C exhibits two sharp Bragg reflection peaks, with a 2θ value of 2.48 (d_1 = 35.34 Å) and 2.88 (d_2 = 30.68 Å), respectively, in addition to a diffuse peak in the wide angle region due to the presence of a large alkoxy terminal chain. In the small angle region, these two sharp reflection peaks can be indexed as (11) and (02), respectively, for a rectangular lattice with two-dimensional lattice parameters calculated as 'a' = 43.23 Å and 'b' = 61.36 Å. These reflections can be explained by the presence of a B1 phase according to Rouillon *et al.* [24].

The X-ray diffraction diagram of **7f** exhibits a sharp peak in the small angle region, with 2θ = 2.48 (d = 35.62 Å) and a broad diffuse peak in the wide angle region centred at d-spacing of 4.64 Å. A diffuse peak in the wide angle region is due to liquid-like correlation of the molecules. The d/L ratio for the compound **7f** is approximately 0.74; this is less than 1 but somewhat

Table 1. The phase transition temperatures and corresponding enthalpy changes of compounds **7a–f.**

Compound 7a:

$$\begin{tikzcd}
\mathrm{Cr} \arrow[r, "92.5", "(8.4)"'] & \mathrm{Cr}_1 \arrow[r, "113.6", "(28.6)"'] & \mathrm{Cr}_2 \arrow[r, "117.5", "(39.7)"'] & \mathrm{B}_2 \arrow[r, "156.2", "(21.3)"'] & \mathrm{I} \arrow[r, "152.3", "(16.9)"'] & \mathrm{B}_2 \arrow[d, "92.0"', "(38.2)"] \\
 & & & & & \mathrm{Cr}
\end{tikzcd}$$

Compound 7b:

$$\mathrm{Cr} \xrightarrow[(21.9)]{109.2} \mathrm{Cr}_1 \xrightarrow[(44.9)]{117.7} \mathrm{B2} \xrightarrow[(22.6)]{156.7} \mathrm{I} \xrightarrow[(22.0)]{156.0} \mathrm{B2} \xrightarrow[(38.7)]{95.9} \mathrm{Cr}$$

Compound 7c:

$$\mathrm{Cr} \xrightarrow[(13.2)]{107.7} \mathrm{Cr}_1 \xrightarrow[(45.1)]{119.9} \mathrm{B2} \xrightarrow[(22.7)]{154.7} \mathrm{I} \xrightarrow[(22.9)]{153.2} \mathrm{B2} \xrightarrow[(40.4)]{98.0} \mathrm{Cr}$$

Compound 7d:

$$\mathrm{Cr} \xrightarrow[(44.1)]{123.5} \mathrm{B1} \xrightarrow[(19.0)]{151.7} \mathrm{I} \xrightarrow[(18.7)]{150.3} \mathrm{B1} \xrightarrow[(28.2)]{95.0} \mathrm{Cr}$$

Compound 7e:

$$\mathrm{Cr} \xrightarrow[(38.5)]{121.7} \mathrm{B1} \xrightarrow[(18.8)]{163.7} \mathrm{I} \xrightarrow[(19.2)]{162.2} \mathrm{B1} \xrightarrow{\qquad} \text{No crystallisation peak found in DSC}$$

Compound 7f:

$$\mathrm{Cr} \xrightarrow[(44.5)]{145.1} \mathrm{B6} \xrightarrow[(19.7)]{195.5} \mathrm{I} \xrightarrow[(19.0)]{194.2} \mathrm{B6} \xrightarrow[(32.5)]{97.6} \mathrm{Cr}$$

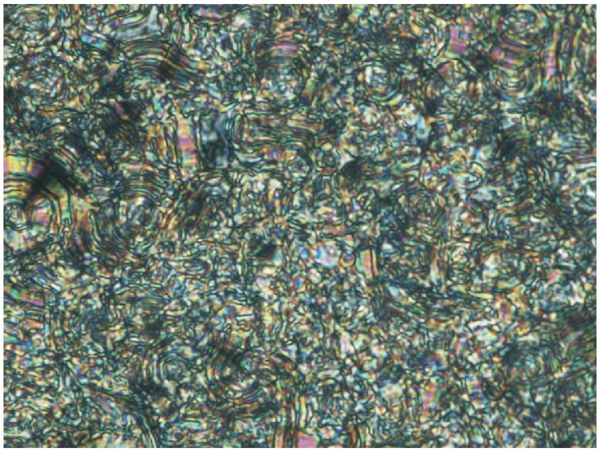

Figure 1. The typical textures of B2 phase of **7b** at 150°C.

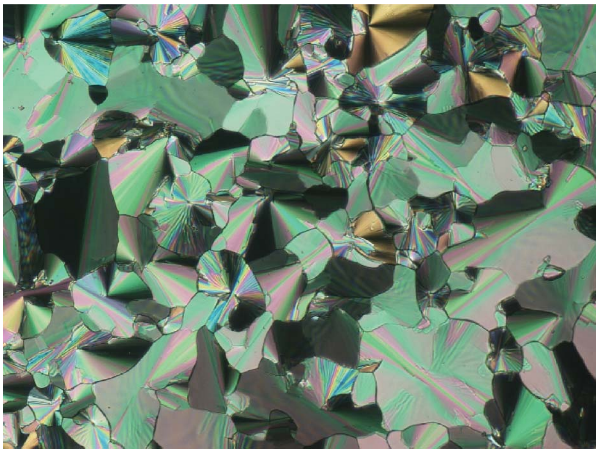

Figure 2. Textures of **7d** at 129°C.

higher than literature reports [22, 25]. This *d*/*L* ratio suggests an intercalated structure. From the X-ray diffraction diagram, molecular modelling and textural observation, the phase of **7f** was identified as B6.

Achard and colleagues [24] reported a series of five ring banana-shaped materials with a thiocarboxy connecting group. In this homologous series (including both lower and higher members), they reported the existence of three mesophases: a B6/B1 dimorphism for lower members; a sole B1 phase for middle members; and a switchable B2 phase for higher members of the homologous series. Reddy and Sadashiva [26] reported three different homologous series of unsymmetrical six-aromatic rings bent-core materials in which one of the terminal position ends with highly polar cyano group and other arms end with an *n*-alkyl chain. They observed a

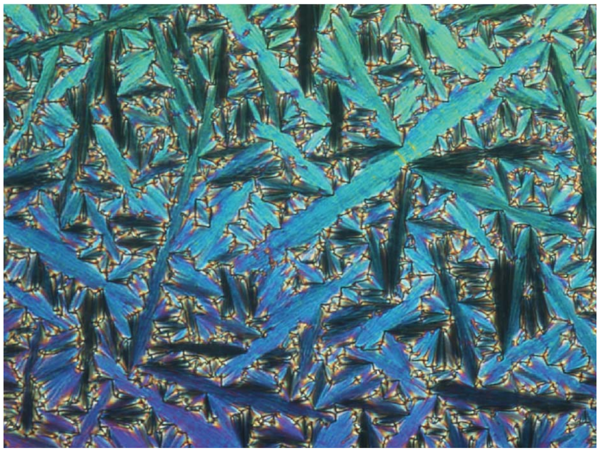

Figure 3. Focal conic textures at 160°C for **7f.**

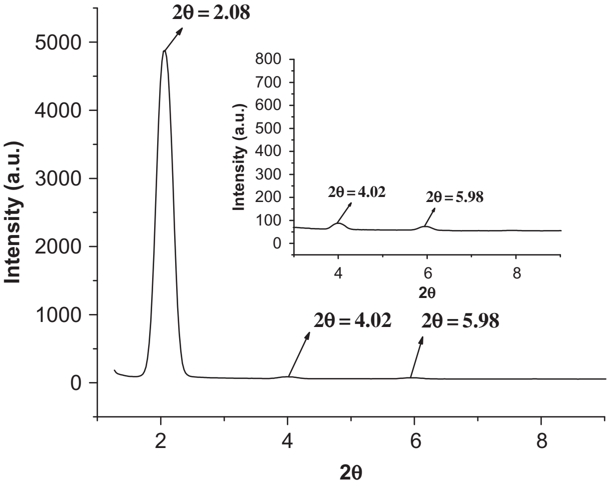

Figure 4. X-ray diffraction diagram of **7b** at 130°C.

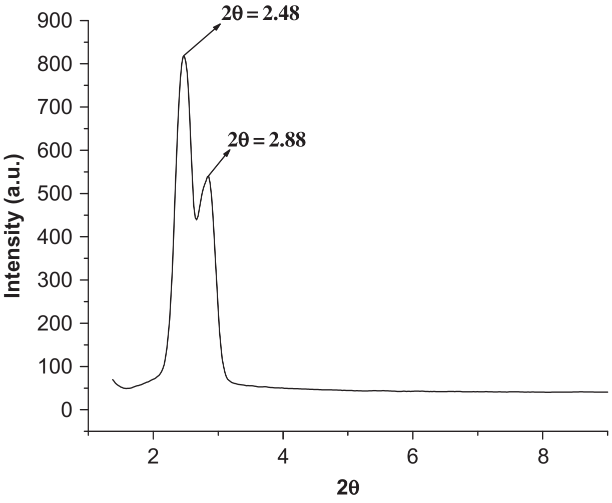

Figure 5. X-ray diffraction diagram of **7d** at 140°C.

transition from nematic phase to polar partial bilayer biaxial smectic A phase. Tschierske's group synthesised six-aromatic ring containing banana-shaped molecules without Schiff's base units which have a ferroelectric switchable liquid crystalline phase [27]. This was achieved by the combination of an angular 3,4′-disubstituted biphenyl central unit with two phenyl benzoate rigid cores via ester linkages. Thus the two halves of these banana-shaped molecules are different. Later the group also synthesised six aromatic ring containing unsymmetrical banana-shaped molecules consisting of rigid angular central units [1,3-disubstituted benzene, 2,7-disubstituted naphthalene, 1,3-diphenylbenzene, 2,6-diphenylnitrobenzene, 2,6-diphenylpyridine, 1,3-bis(phenylethynyl)benzene, 1-phenyl-3-(phenylethynyl)benzene] connected via ester linkages to two rigid cores (1,4-disubstituted benzenes, biphenyl, 2-phenylpyrimidines, phenylbenzoates) [25]. Most of the compounds have higher melting points. Ortega *et al.* [28] synthesised two bent-shaped materials with a biphenyl unit as the central core and observed an extremely rare field-induced transition from B1 to B2.

In this report we have mainly focused on the synthesis and characterisation of six-aromatic ring containing unsymmetrical banana-shaped materials. All the synthesised compounds exhibit mesomorphism. The lower homologue (C_6) displays an intercalated smectic B6 phase. The intermediary homologues (C_{10}, C_{12}) form B1 phase while the mesophase of higher homologues (C_{14}, C_{16}, C_{18}) is characterised as B2.

Acknowledgements

We thank DST (New Delhi) for financial assistance. Two of us (S.C. and P.K.S.) are grateful to CSIR (New Delhi) for their fellowships. We thank Dr Raghunathan of the Raman Research Institute, Bangalore, for providing the HRXRD data. We also thank CMRI, Bhavnagar, for providing X-ray facilities.

References

[1] Demus, D.; Goodby, J.; Gray, G.W.; Spiess, H.-W.; Vill, V. *Handbook of Liquid Crystals*; VCH: Weinheim, 1998.

[2] Lagerwall, S.T.; Dahlgren, A.; Jägemalm, P.; Rudquist, P.; D'havé, K.; Pauwels, H.; Dabrowski, R.; Drzewinski, W. *Adv. Funct. Mater.* **2001**, *11*, 87–94.

[3] Kirsch, P.; Bremer, M. *Angew. Chem., Int. Ed.* **2000**, *39*, 4216–4235.

[4] Niori, T.; Sekine, F.; Watanabe, J.; Furakawa, T.; Takezoe, H. *J. Mater. Chem.* **1996**, *6*, 1231–1233.

[5] Sekine, F.; Niori, T.; Watanabe, J.; Furakawa, T.; Chol, S.W.; Takezoe, H. *J. Mater. Chem.* **1997**, *7*, 1307–1309.

[6] Matsunaga, Y.; Yuri, T. *Mol. Cryst. Liq. Cryst.* **1993**, *237*, 145–150.

[7] Akutagawa, T.; Matsunaga, Y.; Yashahura, K. *Liq. Cryst.* **1994**, *17*, 659–666.

[8] Lee, S.K.; Tokita, M.; Shimbo, Y.; Kang, K.-T.; Takezoe, H.; Watanabe, J. *Bull. Korean Chem. Soc.* **2007**, *28*, 2241–2247.

[9] Gorecka, E.; Pociecha, D. *Phys. Rev. E: Stat., Nonlinear, Soft Matter Phys.* **2000**, *62*, R4524–R4527.

[10] Heppke, G.; Moro, D. *Science* **1998**, *279*, 1872–1873.

[11] Pelzl, G.; Diele, S.; Weissflog, W. *Adv. Mater.* **1999**, *11*, 707–724.

[12] Reddy, R.A.; Tschierske, C. *J. Mater. Chem.* **2006**, *16*, 907–961.

[13] Takezoe, H.; Yoichi, T. *J. Appl. Phys.* **2006**, *45*, 597–625.

[14] Diele, S.; Grande, S.; Kruth, H.; Lischka, Ch.; Pelzl, G.; Weissflog, W.; Wirth, I. *Ferroelectrics* **1998**, *212*, 169–177.

[15] Bedel, J.P.; Rouillon, J.C.; Marcerou, J.P.; Laguerre, M.; Nguyen, H.T.; Achard, M.F. *J. Mater. Chem.* **2002**, *12*, 2214–2220.

[16] Prasad, V.; Kang, S.-W.; Kumar, S. *J. Mater. Chem.* **2003**, *13*, 1259–1264.

[17] Keith, C.; Reddy, R.A.; Hahn, H.; Lang, H.; Tschierske, C. *Chem. Commun.* **2004**, 1898–1899.

[18] Yelamaggad, C.V.; Shashikala, I.S.; Hiremath, U.S.; Liao, G.; Jakli, A.; Rao, D.S.S.; Prasad, S.K.; Li, Q. *Soft Matter* **2006**, *2*, 785–792.

[19] Majumdar, K.C.; Chattopadhyay, B.; Chakravorty, S.; Pal, N.; Sinha, R.K. *Tetrahedron Lett.* **2008**, *49*, 7149–7152.

[20] Majumdar, K.C.; Chakravorty, S.; Pal, N. *Mol. Cryst. Liq. Cryst.* **2009**, *50*, 112–125.

[21] Majumdar, K.C.; Chakravorty, S.; Sinha, R.K.; Pal. N. *Mol. Cryst. Liq. Cryst.* **2009**, *515*, 123–132.

[22] Pelzl, G.; Diele, S.; Weissflog, W. *Adv. Mater.* **1999**, *11*, 707–724.

[23] Bedel, J.P.; Rouillon, J.C.; Marcerou, J.P.; Laguerre, M.; Achard, M.F.; Nguyen, H.T. *Liq. Cryst.* **2000**, *27*, 103–113.

[24] Rouillon, J.C.; Marceron, J.P.; Laguerre, M.; Nguyen, H.T.; Achard, M.F. *J. Mater. Chem.* **2001**, *11*, 2946–2950.

[25] Shen, D.; Diele, S.; Wirth, I.; Tschierske, C. *J. Mater. Chem.* **1999**, *9*, 661–672.

[26] Reddy, R.A.; Sadashiva, B.K. *J. Mater. Chem.* **2004**, *14*, 310–319.

[27] Shen, D.; Diele, S.; Wirth, I.; Tschierske, C. *Chem. Commun.* **1998**, 2573–2574.

[28] Ortega, J.; De la Fuente, M.R.; Etxebarria, J.; Folcia, C.L.; Dıez, S.; Gallastegui, J.A.; Gimeno, N.; Ros, M.B.; Perez-Jubindo, M.A. *Phys. Rev. E: Stat., Nonlinear, Soft Matter Phys.* **2004**, *69*, 011703–7.